Am J Nucl Med Mol Imaging 2016;6(1):59-72
www.ajnmmi.us /ISSN:2160-8407/ajnmmi0016804

Original Article

^{68}Ga-DOTATOC PET and gene expression profile in patients with neuroendocrine carcinomas: strong correlation between PET tracer uptake and gene expression of somatostatin receptor subtype 2

Ingrid H Olsen[1,2,3,4,5,6], Seppo W Langer[1,5], Birgitte H Federspiel[1,6], Jytte Oxbøl[1,2], Annika Loft[1,2], Anne Kiil Berthelsen[1,2], Jann Mortensen[1,2], Peter Oturai[1,2], Ulrich Knigge[1,2,3,4], Andreas Kjær[1,2]

[1]European NET Centre of Excellence, Rigshospitalet, University of Copenhagen, Denmark; [2]Department of Clinical Physiology, Nuclear Medicine & PET and Cluster for Molecular Imaging, Rigshospitalet and University of Copenhagen, Denmark; Departments of [3]Endocrinology, [4]Surgical Gastroenterology, [5]Oncology, [6]Pathology, Rigshospitalet, University of Copenhagen, Denmark

Received September 24, 2015; Accepted December 4, 2015; Epub January 28, 2016; Published January 30, 2016

Abstract: Somatostatin receptor expression on both protein and gene expression level was compared with *in vivo* ^{68}Ga-DOTATOC PET/CT in patients with neuroendocrine carcinomas (NEC). Twenty-one patients with verified NEC who underwent a ^{68}Ga-DOTATOC PET/CT between November 2012 and May 2014, were retrospectively included. By real-time polymerase chain reaction, we quantitatively determined the gene expression of several genes and compared with ^{68}Ga-DOTATOC PET uptake. By immunohistochemistry we qualitatively studied the expression of assorted proteins in NEC. The median age at diagnosis was 68 years (range 41-84) years. All patients had WHO performance status 0-1. Median Ki67 index was 50% (range 20-100%). Gene expression of somatostatin receptor subtype (SSTR) 2 and Ki67 were both positively correlated to the ^{68}Ga-DOTATOC uptake ($r=0.89$; $p<0.0001$ and $r=0.5$; $p=0.021$, respectively). Furthermore, SSTR2 and SSTR5 gene expression were strongly and positively correlated ($r=0.57$; $p=0.006$). This study as the first verifies a positive and close correlation of ^{68}Ga-DOTATOC uptake and gene expression of SSTR2 in NEC. SSTR2 gene expression has a stronger correlation to ^{68}Ga-DOTATOC uptake than SSTR5. In addition, the results indicate that the gene expression levels of SSTR2 and SSTR5 at large follow one another.

Keywords: Neuroendocrine carcinoma, neuroendocrine tumors, immunohistochemistry, gene expression, imaging, ^{68}Ga-DOTATOC PET/CT, somatostatin receptor type 2, somatostatin receptor type 5, mammalian target of rapamycin, urokinase-type plasminogen activator receptor

Introduction

Neuroendocrine neoplasms (NENs) are defined as epithelial tumors with predominant neuroendocrine differentiation and an expression of general neuroendocrine tumor markers as chromogranin A (CgA) and synaptophysin. The World Health Organization (WHO) 2010 classification of gastroenteropancreatic (GEP)-NENs is based on proliferation (Ki67 index and mitotic count), opposed to the NEN classification of the lung utilizing mitotic count [1-4].

GEP-NENs with Ki67 >20% are classified as the high-grade neuroendocrine carcinomas (NECs, WHO grade (G) 3) and constitute a heterogeneous group. NECs are a contentious topic since the diagnosis, prognostic markers and therapeutic options have been challenged [5, 6]. Despite increasing research on NECs, the median overall survival (OS) is stagnant. Disseminated NEC is primarily treated with chemotherapy [7]. Platinum-based chemotherapy is established as first line treatment, yet patients with GEP-NEC have a poor OS even on treatment (4-16 months) and new therapeutic alternatives are warranted [6-8]. Patients with high-grade lung NEN have a median OS of 17 months, and the prognosis for patients with primary thymic NEN remains poor, patients having a 5-year survival of nearly 0% [2]. Moreover, the Nordic NEC study showed that the objective response

rate was lower in patients with GEP-NEC having a Ki67 index <55% compared to patients with a Ki67 index ≥55% supporting the concept that the current WHO G3 category is heterogeneous [7]. Supplementary characterization of NECs is essential for selection of patients with response to therapy.

Functional imaging and histopathology may be important for diagnosis, selection of treatment, and prediction of prognosis in patients with NEC. Somatostatin (SST) is a peptide present in neurons and endocrine cells with an inhibitory effect on a wide range of physiological functions [9]. Furthermore, SST has an important regulatory role in neurotransmission and secretion. Its anti-proliferative action in normal tissues and in NENs has the ability to control cell growth with the potential for therapeutic application [9-12]. SST actions are mediated by transmembrane domain G-protein-coupled receptors, yet the signaling pathway of SST is complex and varies among receptors types, cells and organs. Six distinct subtypes of somatostatin receptors (SSTR) are identified (SSTR 1, 2A, 2B, 3, 4 and 5). SSTR2B has not been identified in humans [13]. Multiple subtypes may frequently coexist in the same cell [14]. Naturally occurring SST has a very low metabolic stability *in vivo* (<2 minutes) and more stable synthetic analogues have therefore been developed for treatment and *in vivo* diagnostic purposes labeled with positron emitters as fluorine-18 (^{18}F), copper-64 (^{64}Cu) and gallium-68 (^{68}Ga) [14-17]. Somatostatin receptor imaging (SRI) is so far the most specific and sensitive imaging modality for NENs [18].

Particularly, NENs with a Ki67 index ≤20% (WHO G1 and G2) have an overexpression of membrane bound SSTR, which can be targeted with radiolabeled analogues [9, 14, 19]. Available agents include the 1,4,7,10-tetraazacyclododecane-1,4,7,10-tetraacetic acid (DOTA)-coupled, SST-based radiopeptides [DOTA^0, Tyr^3]-octreotide (DOTATOC) and [DOTA^0, Tyr^3, Thr^8]-octreotide (DOTATATE) [18]. ^{68}Ga-DOTATOC is a SST-based ligand for positron emissions tomography (PET)/computed tomography (CT) which predominately binds SSTR2 [14]. The expression pattern of SSTRs in NENs has been studied by semi-quantitative approaches and molecular imaging based on radioactive labeling of SST analogs, and has gained a pivotal role in the diagnostic workup of NENs [10, 14, 19-21]. However, the gene expression pattern of SSTRs and ^{68}Ga-DOTATOC has to the best of our knowledge never been studied in NECs.

The aim of the study was to obtain a more accurate identification of the quantitative gene expression underlying ^{68}Ga-DOTATOC results in NECs, which has not previously been established and to elucidate whether the expression of SSTR2 and SSTR5, could explain the results obtained by ^{68}Ga-DOTATOC PET. Therefore, by real-time polymerase chain reaction (qPCR), we quantitatively determined the gene expression of several genes. In addition, we qualitative studied the expression of assorted proteins by immunohistochemistry (IHC) in NEC.

Material and methods

Patient identification

Twenty-one patients with a histopathologically verified NEC, who underwent a ^{68}Ga-DOTATOC PET/CT between 7th of November 2012 and 20th of May 2014, were retrospectively included at Department (Dept.) of Surgical Gastroenterology, Dept. of Oncology, Dept. of Endocrinology and Dept. of Clinical Physiology, Nuclear Medicine and PET at Rigshospitalet, Denmark. Data processing was handled in a non-personalized matter (patient-numbering). As a retrospective database study the National Committee on Health Research Ethics did not require written or verbal informed consent. The NEN-database of Rigshospitalet was approved by The Danish Data Protection Agency (#2007-58-0015), and data extracted from here. The study was performed in accordance with the Declaration of Helsinki.

Immunohistochemistry

Formalin-fixed paraffin-embedded (FFPE) tissue from all 21 patients was available either from primary tumors (13 patients) or metastases (8 patients). The tissue in 11 cases was from biopsies. IHC was performed on all tissue specimens to assess potential makers for characterization using the antibodies summarized in **Table 1A**. The FFPE tissue was cut in 4 µm thick section, mounted on glass slides, and placed in an incubator at 40°C for 60 minutes. The temperature was increased for one hour and 15 minutes to 60°C, and the slides were

Table 1A. Antibodies used for immunohistochemistry

Antibody	Clone/Code	Host	Provider	Dilution
Ki67	MIB1	Monoclonal Mouse	Dako Denmark A/S, Glostrup, DK	1:100
uPAR	R2	Monoclonal Mouse	Finsen in-house	1:20000
Anti-SSTR2	8B44	Monoclonal Mouse	My Biosource, San Diego, USA	1:150
SSTR5	SP4678P	Polyclonal Rabbit	Acris Antibodies, Herford, Germany	1:200
Anti-mTOR	ab25880	Polyclonal Rabbit	Abcam, Cambridge, USA	1:1000
Synaptophysin	Svp 88	Monoclonal Mouse	Novestra Ltd, Newcastle, UK	1:50
Chromogranin A	A0430	Polyclonal Rabbit	Dako Denmark A/S, Glostrup, DK	1:2000

Table 1B. Primer identification, sequences, amplicon length and concentration for the genes investigated

Genes	NM ID	Forward Primer (5'-3')	Reverse Primer (5'-3')	Amplicon length bp	Forward primer Final conc. nmol/L	Reverse primer Final conc. nmol/L
References						
ACTB	001101	TGGCATCCACGAAAACTAC	GGCAGTGATCTCCTTCTG	142	300	300
PPIA	021130	CGGATTTGATCATTTGGTG	CCAGACAACACACAAGAC	109	300	300
B2M	004048	CCAAAGATTCAGGTTTACTC	CAACTTCAATGTCGGATG	100	600	300
YWHAZ	001135700	AACTGCTTCCATGTCTAA	TTACTACACCTGTGACTG	97	600	300
GAPDH	001289746	GTCGGAGTCAACGGATTT	GCAACAATATCCACTTTACCA	80	600	300
Targets						
VEGF-a	001025366	GAGTGGTTGACCTTCC	GGGATATTAAATAAGTACCGTATA	138	300	300
ITGAV	002210	GGGTCAAGATCAGTGAGAAATCTTTAC	ATTCCTGTAACATCATGCTATTGCTAG	139	300	600
ITGB3	00212	CTCCTGTCCCTCATCCATAGC	CAGCCAAGAGGTAGAAGGTAAATAC	103	300	300
CAIX	001216	CTGCCCTCTGACTTCA	CAGAGAGGGTGTGGAG	133	300	300
HIF1-a	181054	AGCAGTCTATTTATATTTTCTACA	GAGCATTAATGTAAATTAAGTAGA	111	300	300
SSTR2	001050	ACCTCGTATAAGCTTCAAG	GGTTCTTCAAATATCTTCTTC	121	600	600
SSTR5	001172560	CTGAGTGGGCACAAATCC	ATTTATCCTCGCATTTATTCAG	121	300	600
uPAR	001005376	GCTGCCTGTGATAAATTATTAC	CTCCCAAAGTGCTAGGAC	116	300	300
mTOR	004958	GATAAGCTCACTGGTCGG	AATATAGCACTGGCAGAGG	114	300	300
Ki67	002417	TCCCGCCTGTTTTCTTTCTGAC	CTCTCCAAGGATGATGATGCTTTAC	121	600	600

deparaffinized in shifts of xylene for 15 minutes followed by multiple shifts of ethanol in decreasing concentrations from 99.9% advancing the sections to demineralized water. Antigen retrieval was performed using heat-induced epitope retrieval (HIER) in citrate buffer pH 6.0 for 15 minutes in a microwave oven followed by 30 minutes rest at room temperature and then immersion in phosphate-buffered saline (PBS) containing 0.1% TWEEN®20 (cat. #P1379-25 mL, Sigma-Aldrich, St. Louis, Missouri (MO), USA) for five minutes. Subsequent reactions all took place at room temperature. After 10 minutes of immersion in PBS, the slides were transferred to humidity chambers where each section was covered with peroxidase blocker (cat. #S2023, Dako, Glostrup, Denmark) for eight minutes and then rinsed with three shifts of PBS every two minutes. The sections were blocked using 2% Bovine Serum Albumin (BSA) (cat. #A7906-100g, Sigma-Aldrich, St. Louis, MO, USA) for 10 minutes followed by primary antibody diluted in 2% BSA for samples and positive control tissue, whereas species-matched FLEX control (cat. #IS600 [rabbit] and #IS750 [mouse], Dako, Glostrup, Denmark) was added to negative control samples. Antibody dilutions are described in **Table 1A**. The samples were then incubated for one hour followed by rinse in three shifts of PBS every two minutes.

The secondary horseradish peroxidase conjugated antibody was now added to the samples; EnVision™ FLEX (cat. #K4001 [mouse], Dako, Glostrup, Denmark), which was left, to incubate for another 40 minutes followed by rinse in two shifts of PBS for five minutes. The samples were developed using 3,3'-diaminobenzidine (DAB) for 10 minutes (cat. #K3468, Dako,

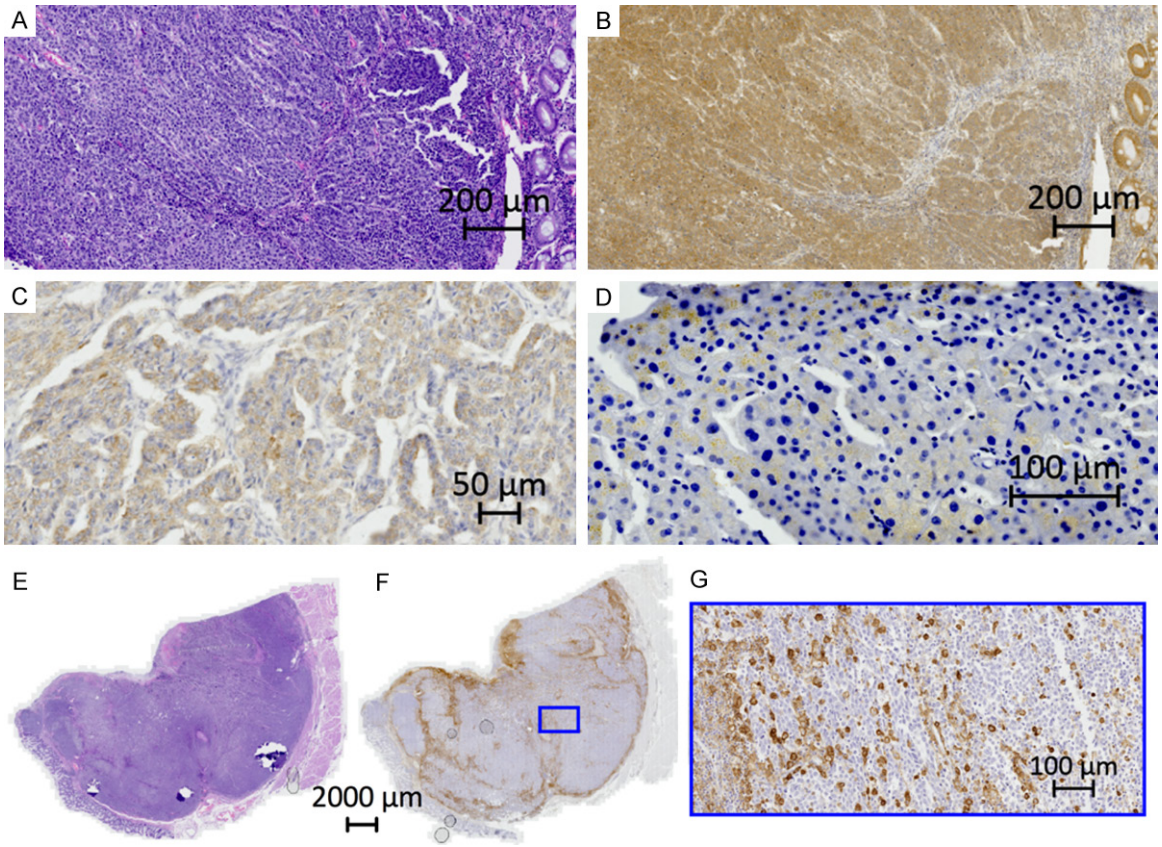

Figure 1. Immunohistochemical images. A. HE. Large cell neuroendocrine carcinoma from the right colon. B. Same tumor as in A. SSTR2. Score 3. Circumferential membranous reactivity. C. SSTR5. Poorly differentiated large cell neuroendocrine carcinoma metastasis from the ovary. Cancer of unknown primary (CUP). Cytoplasmic staining. D. mTOR. Large cell neuroendocrine carcinoma metastasis from the liver. Cytoplasmic staining. E. HE. Large cell neuroendocrine carcinoma from the rectum. F. Same tumor as in F. uPAR. Score 2. Stromal and circumferential reactivity. G. Zoom of F.

Glostrup, Denmark) followed by rinse in PBS for two minutes. The samples were transferred to soak in demineralized water for five minutes, counterstained by one minute of Mayer's hematoxylin, soaked for five minutes in demineralized water, before being dehydrated in ethanol and finally mounted using PERTEX® as a mounting medium.

Slides were scanned using an Axio Scan.Z1 slide scanner (Carl Zeiss Microscopy GmbH, Jena, Germany) and subsequent image preparation was performed using software Zen lite, Carl Zeiss.

Interpretation of IHC results

Ki67 immunoreactivity was expressed as the mean percentage of tumor cells with the highest nuclear labeling after manual counting of 20 hot spot areas. CgA immunoreactivity was scored as positive (>30% of the tumor cells reacted), focally positive (1-30% of the tumor cells reacted) or negative (less than 1% of the tumor cells reacted). All specimens had a positive immunoreaction for synaptophysin (>70% of the tumor cells reacted).

For SSTR2 a semi-quantitative scoring system, validated in previous publication was used, taking into consideration both the subcellular localization and the extent of the staining, as follows [22]. Score 0: absence of immunoreactivity; score 1: pure cytoplasmic immunoreactivity, either focal or diffuse; score 2: membranous reactivity in less than 50% of tumor cells, irrespective of the presence of cytoplasmic staining; score 3: circumferential membranous reactivity in more than 50% of tumor cells, irrespective of the presence of cytoplasmic staining (**Figures 1A**, **1B**, **2**, **Table 2**) [22].

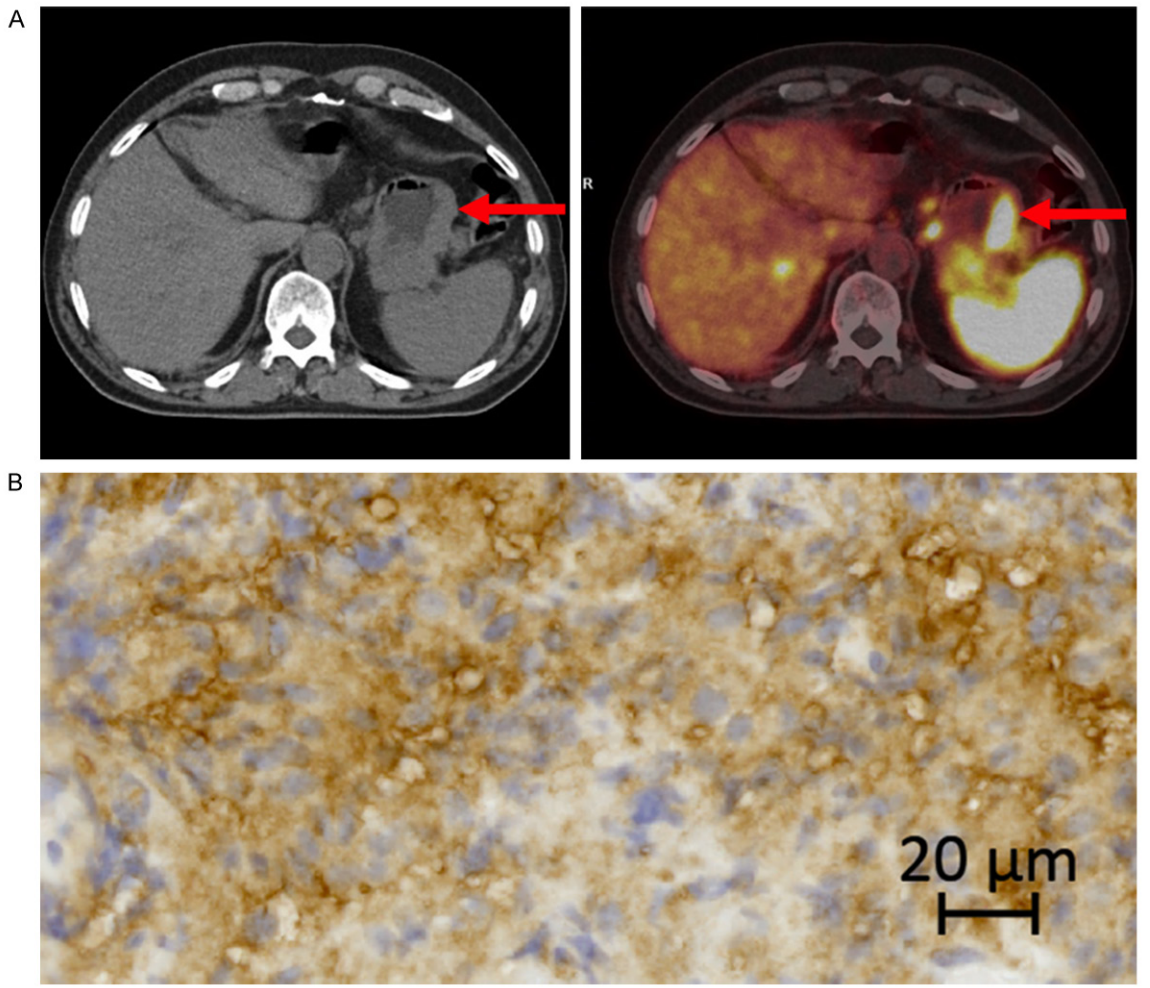

Figure 2. A. ^{68}Ga-DOTATOC PET/CT of a neuroendocrine carcinoma in the stomach (arrows) with high SSTR2 gene expression. B. IHC of same tumor as in A. SSTR2 score 2.

For SSTR5 a cytoplasmic pattern of staining was observed, and cases were scored as positive in the presence of at least 10% of positive tumor cells, an interpretation validated in earlier publication (**Figure 1C**, **Table 2**) [22].

Several scoring systems for immunoreactivity of mamalian target of rapamycin (mTOR), have been suggested, both semi-quantitative (immunoreactive score (IRS), H-score) and dichotomization in positive and negative staining [23-30]. In the present study a cytoplasmic pattern of staining in tumor cells was observed in only 3 cases the remainder were negative, hence cases were scored as positive in the presence of at least 30% of positive tumor cells (**Figure 1D**, **Table 2**).

The monoclonal antibody (R2) against human urokinase-type plasminogen activator receptor (uPAR) has been described previously [31]. Semi-quantitative scoring systems for uPAR have earlier been described, optimized and tested [32, 33]. As well as a simplified scoring system of uPAR [34-36]. Suitable for the present cohort the immunoreactivity was scored as follows: 0: no uPAR positive cells; 1: only uPAR positive stromal cells in tumor; 2: uPAR positive stromal and circumference of tumor plus above 10% positive tumor cells (**Figure 1E-G**, **Table 2**). Hematoxylin-eosin (HE) slides were morphologically evaluated as small or large cell [1].

Quantitative real time polymerase chain reaction (qPCR)

RNA extraction from FFPE: Tissue blocks were cut in 2×10 µm thick sections that were put into a 1.5 ml sterile Sarstedt tube® (Sarstedt AG & Co., Nümbrecht, Germany). Tissue sections

Table 2. Patient and disease characteristics (n=21)

Number of females	11 (52%)
Number of males	10 (48%)
Age at scanning time (median (yrs), range)	68 (41-84)
WHO performance status at scanning time	
1	13 (62%)
0	8 (38%)
Location of primary tumor	
Esophagus or stomach	3 (14%)
Small Intestine	1 (5%)
Colo-rectal	6 (29%)
Pancreas	4 (19%)
Thymus	1 (5%)
Lung	3 (14%)
*CUP**	3 (14%)
Metastatic disease**	
Lymph node metastases	11 (52%)
Liver metastases	11 (52%)
Bone metastases	2 (10%)
Brain metastases	3 (14%)
Immunohistochemistry	
Ki67 (median (%), range)	50 (20-100)
Ki67<55%	11 (52%)
Ki67≥55%	10 (48%)
Chromogranin A	
Positive	10 (48%)
Focally positive	9 (43%)
Negative	2 (10%)
Synaptophysin positive	21 (100%)
SSTR2	
3 (circumferential membranous reactivity ≥50% of tumor cells, irrespective of the presence of cytoplasmic staining)	3 (14%)
2 (membranous reactivity in <50% of tumor cells, irrespective of the presence of cytoplasmic staining)	4 (19%)
1 (pure cytoplasmic immunoreactivity, either focal or diffuse)	10 (48%)
0 (negative)	2 (10%)
not done	2 (10%)
SSTR5	
Positive (>10% pos. cells, cytoplasmic)	8 (38%)
Negative	9 (43%)
Not done	4 (19%)
m-TOR	
Positive	3 (14%)
Negative	17 (81%)
Not done	1 (5%)
uPAR	
2: stromal and circumferences and >10% positive tumor cells	10 (48%)
1: only stromal cells	6 (29%)
0: no uPAR positive cells, negative	3 (14%)
not done	2 (10%)

*Cancer of unknown primary. **Metastatic disease verified by surgery, CT or pathology.

were deparaffinized and RNA extracted using the Tissue Preparation System (Siemens Healthcare Diagnostics Inc., Tarrytown, USA). The RNA samples were stored at -80°C until further analysis.

cDNA synthesis: Using the AffinityScript™ QPCR cDNA Synthesis Kit (cat. #600559 Stratagene, La Jolla, CA, USA), 0.022 µg of total RNA was reverse transcribed to cDNA. RNA Sample quantity was assessed using a NanoDrop spec-

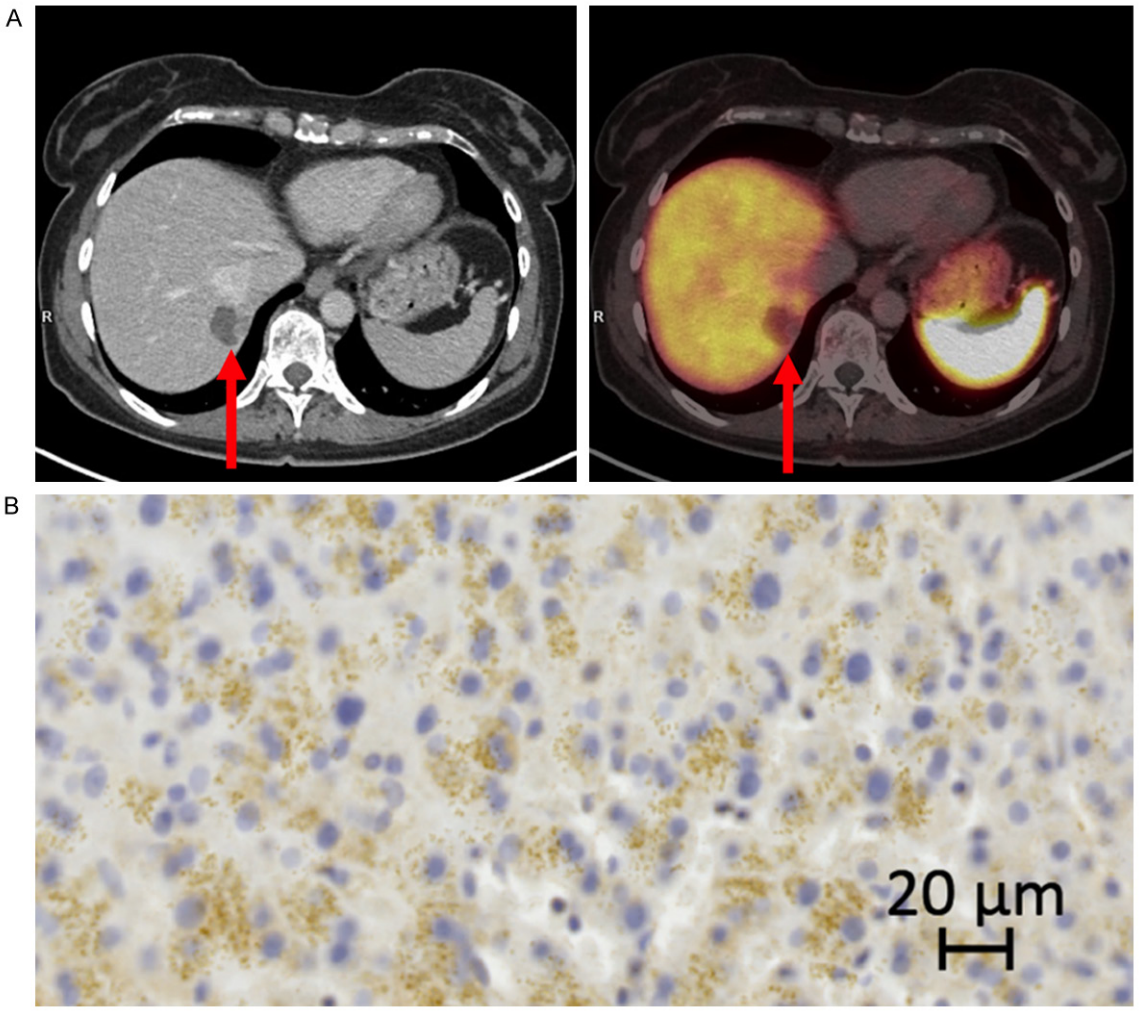

Figure 3. A. ^{68}Ga-DOTATOC PET/CT of a liver metastasis (arrows) with low SSTR2 gene expression from a gastric neuroendocrine carcinoma. B. IHC of the same liver metastasis as in A. SSTR2 score 1.

trophotometer (Thermo Fisher Scientific, Waltham, MA, USA). Subsequent real-time qPCR analysis and the procedures were performed according to the protocol of the manufacturer. In brief: A mixture containing 7 µL (0.022 µg) total RNA, 10 µL first strand master mix (2x), 2.45 µL Oligo (dT) primer (0.1 µg/µL), 0.55 µL random primer (0.1 µg/µL) and 1 µL of Stratascript™ RT/RNase Block Enzyme Mixture were prepared and run on a Mastercycler gradient PCR machine (Eppendorf AG, Hamburg, Germany) utilizing a program of 5 minutes of primer annealing at 25°C, 15 minutes of cDNA synthesis at 42°C and finally termination for 5 minutes at 95°C. Subsequently cDNA was stored at -20°C until qPCR analysis.

Quantitative real-time PCR: Tumor tissue from 12 NEN patients was tested, using a commercially available panel ("Human Endogenous Control Gene Panel") of 12 reference genes (cat. #A101, Version 1.3 TATAA Biocenter AB, Göteborg Sweden). Five reference genes (RGs) (**Table 1B**) were found to be optimal using the geNorm algorithm embedded in the qBase^{+} software (Biogazelle NV, Zwijnaarde, Belgium) [37]. The RG stability was 0.957 (M-value) and 0.417 (CV-value), reflecting the heterogeneity of the sample panels, since CV and M values <25% and 0.5, respectively, are observed in relatively homogeneous sample panels [37].

Primers for the genes of interest (GOI) and the five chosen most stably expressed RGs were designed using Beacon Designer™ 7.90 (PREMIER Biosoft, Palo Alto, CA, USA) and quantified using Mx3005P™ real-time PCR system (Stratagene, La Jolla, CA, USA). All primer

Table 3. Correlation of the ten genes of interest and ^{68}Ga-DOTATOC uptake

Genes of interest (GOI)*	$SUV_{max\ biopsy}$*	
	Pearson's r (95% CI)	*p*-value
SSTR2	0.89 (0.74-0.95)	<0.0001
SSTR5	0.4 (-0.03-0.71)	0.07
ITGAV	-0.02 (-0.45-0.42)	0.932
ITGB3	0.05 (-0.39-0.47)	0.834
Ki67	0.5 (0.09-0.77)	0.021
uPAR	0.09 (-0.35-0.50)	0.694
VEGFA	-0.08 (-0.50-0.36)	0.72
mTOR	0.42 (-0.01-0.72)	0.055
HIF1α	0.25 (-0.19-0.62)	0.248
CA-IX	0.25 (-0.19-0.62)	0.25

*Log_{10}; n=21.

designs included a BLAST search for test of homology and a test for secondary structures. The chosen primers were optimized to determine the final concentrations for the PCR, using reference cDNA from Human Reference RNA, Stratagene cat. #750500 (**Table 1B**). All primers were purchased from Sigma (Sigma-Aldrich, St. Louis, MO, USA).

Ten GOI were analyzed (**Table 1B**). All samples were run in duplicates using 1 µL cDNA. The Brilliant III Ultra-Fast SYBR® Green Master Mix (Stratagene, cat. #600882) was used. The thermal profile consisted of an initial denaturation at 95°C for 3 minutes followed by 40 cycles of denaturation at 95°C for 20 seconds and an annealing/extention step at 60°C for 20 seconds. Gene expression data analysis was performed in qBase+ software (Biogazelle NV, Zwijnaarde, Belgium) [37]. An amplification efficiency of 100% was used for all targets and data was reported as normalized relative quantities (NRQs). The normalization factor of the five RGs was calculated and used for normalization of the samples as described previously [38].

^{68}Ga-DOTATOC PET/CT

Labeling technique and quality control of the radiopharmaceutical was performed according to the method described in a previous publication [39]. In brief: All patients underwent PET/CT-scans with ^{68}Ga-DOTATOC on dedicated PET/CT scanners (Siemens Biograph™ True Point™, Siemens mCT, Siemens, Erlangen, Germany). A dose of 150 MBq ^{68}Ga-DOTATOC was injected intravenously and, after 45 minutes, whole-body PET was performed. On the same scanner, CT scans were performed immediately prior to the PET scan. All CT scans were acquired as a high quality diagnostic CT scan with the use of intravenous contrast unless contraindications. The PET scan followed immediately with an acquisition time of 3 min per bed position. The CT data were used for attenuation correction of the PET data. Both image sets were reconstructed in trans-axial, coronal and sagittal images with a slice thickness of 5 mm and 3 mm. Maximum standardized uptake value $(SUV)_{max}$ in pathological foci as well as normal tissue was measured (**Figures 2** and **3**). $SUV_{max\ biopsy}$ was obtained by drawing spherical volumes of interest sufficiently large to encompass the whole lesion, hence a rim of surrounding normal tissue was included. $SUV_{max\ biopsy}$ reflected the specific uptake in the organ from where the biopsy was taken and used for further IHC and gene expression analyses.

Statistical analysis

Logarithmic transformation (log_{10}) of the gene expression data and $SUV_{max\ biopsy}$ were applied to obtain normal distribution. Normal distribution assumptions were tested using the Kolmogorov-Smirnov test. PET data and gene expression analyses were compared using the Pearson correlation coefficient as appropriate. P<0.05 was considered statistically significant. Analyses were performed using SPSS 22 (IBM Corporation, Armonk, New York, USA).

Results

Patient characteristics

The clinicopathological characteristics of the 21 patients are summarized in **Table 2**. The median age at scanning time was 68 years (41-84 years). All patients had WHO performance status 0-1.

Morphology and immunohistochemistry (IHC)

Morphologically, 3 (14%) were categorized as small cell, the remaining as large cell. Median Ki67 index was 50% (range 20-100%). Four patients included in our study had a Ki67 at the cut-off point for G3 (Ki67=20%). According to the findings in the Nordic NEC study, patients were categorized as Ki67 20-55% (n=11; 52%) and Ki67≥55% (n=10; 48%) (**Table 2**). The allo-

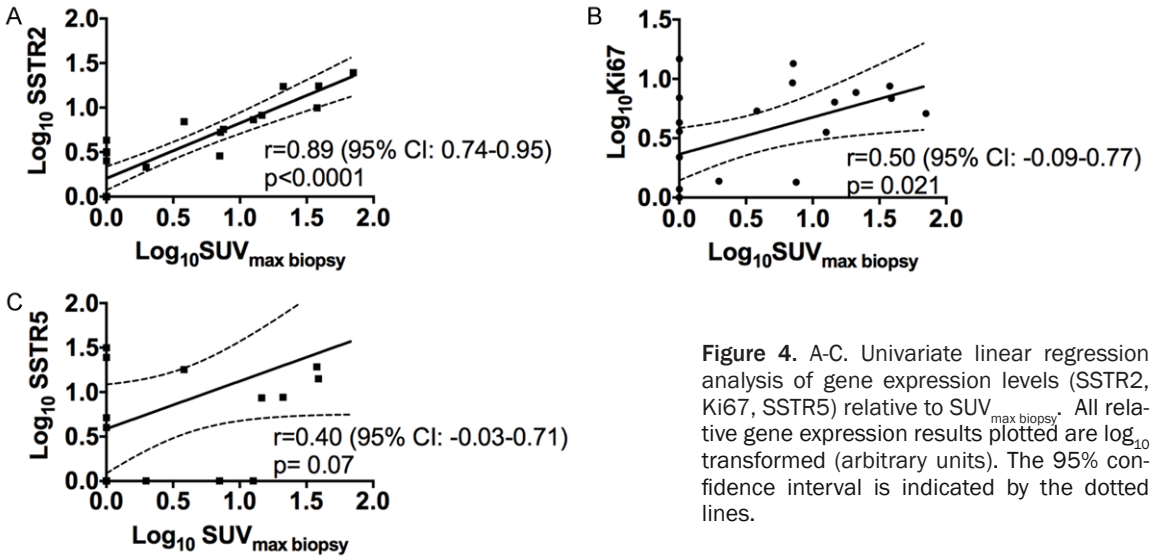

Figure 4. A-C. Univariate linear regression analysis of gene expression levels (SSTR2, Ki67, SSTR5) relative to $SUV_{max\ biopsy}$. All relative gene expression results plotted are log_{10} transformed (arbitrary units). The 95% confidence interval is indicated by the dotted lines.

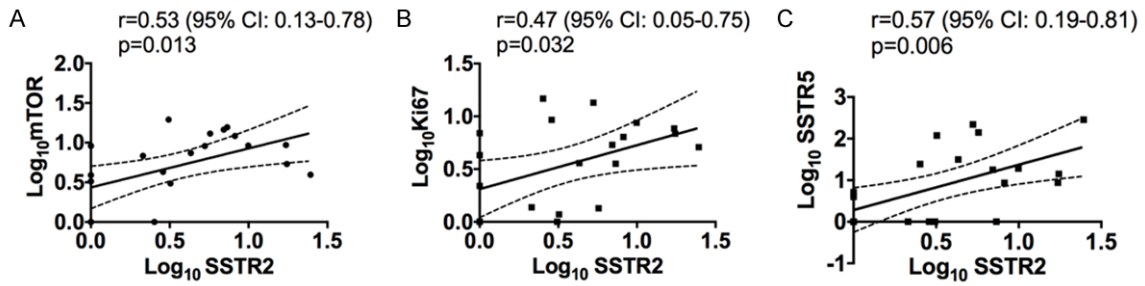

Figure 5. A-C. Univariate linear regression analysis of SSTR2 gene expression relative to mTOR-, Ki67- and SSTR5 gene expression. All relative gene expression results plotted are log_{10} transformed (arbitrary units). The 95% confidence interval is indicated by the dotted lines.

cation of the semi-quantitative assessment of the various IHC markers is depicted in **Table 2** and illustrated in **Figure 1**.

Gene expression and correlation with ^{68}Ga-DOTATOC

The $SUV_{max\ biopsy}$ values were correlated to gene expression levels of all GOI, **Table 3**. SSTR2 and Ki67 were both statistically significant, positively correlated to the ^{68}Ga-DOTATOC-uptake (r=0.89; p<0.0001 and r=0.5; p=0.021, respectively) (**Figure 4**). A trend towards a positive correlation between ^{68}Ga-DOTATOC-uptake and mTOR (r=0.42; p=0.055) and SSTR5 (r=0.4; p=0.070; **Figure 4**) was found.

Prompted by the correlation between SSTR2 gene expression and $SUV_{max\ biopsy}$, the relation of SSTR2 gene expression to SSTR5, Ki67 and mTOR gene expression was also investigated and shown in **Figure 5**. Most notable was the strong positive correlation of SSTR2 and SSTR5 relative gene expression (r=0.57; p=0.006). Gene expression of Ki67 and mTOR were also significantly correlated to gene expression of SSTR2 (r=0.47; p=0.032 and r=0.53; p=0.013) (**Figure 5**).

Discussion

To our knowledge this is the first study comparing qPCR data for SSTR2 and SSTR5 in NECs with ^{68}Ga-DOTATOC PET/CT results. The major finding of the present study was a strong correlation between ^{68}Ga-DOTATOC uptake and SSTR2 gene expression as assessed by qPCR (p<0.0001). The expression of gene level of SSTR2 compared to SSTR5 was positively correlated (p=0.006), yet the results depicted in **Figure 4** reflect that SSTR2 gene expression was stronger correlated to ^{68}Ga-DOTATOC uptake than SSTR5 (p<0.0001 and p=0.07, respectively). The results indicate that the gene

expression levels of SSTR2 and SSTR5 follow one another, however, suggesting SSTR2 to be of highest impact for the PET signal. Previous studies found the relative level of gene expression in NEN to be much higher for SSTR2 than for any of the other SSTR subtypes [20, 40]. The most used ^{68}Ga- and ^{64}Cu-labeled somatostatin receptor ligands (^{68}Ga-DOTANOC, ^{68}Ga-DOTATATE, ^{68}Ga-DOTATOC and ^{64}Cu-DOTATATE) differ in affinity for the SSTR2. Furthermore, ^{68}Ga-DOTANOC has higher affinity toward SSTR5, nevertheless clinical data show no major difference in performance [41]. Accordingly, it is no surprise that SSTR2 gene expression and not SSTR5 gene expression is the major determinant for PET tracer binding. Yet, for longitudinal comparison the use of the same ^{68}Ga-based tracers may be important, e.g. due to differences in background uptake [41].

It could be argued, that gene expression does not necessarily lead to protein synthesis. However, since we found such a strong correlation in the present study it seems that gene expression did reflect the synthesis of SSTR2 in NEC. This is important for future studies, as qPCR is an easy and truly quantitative method than can then be used for prediction of SRI outcome.

An earlier study comparing material from fresh-frozen tissue samples with FFPE tissue, showed that fresh-frozen tissue performed better in terms of the level of amplification, but acceptable and concordant results were also obtained from FFPE samples [28]. However, in our study we found that also FFPE samples can be used for study of gene expression as no strong correlation would otherwise had been found.

Gene expression of the proliferation-associated gene, Ki67, correlated positively to gene expression of SSTR2 ($p=0.032$) and SRI uptake ($p=0.021$) (**Figures 4** and **5**). We would expect a negative correlation, since SRI is less frequently positive in patients with a high Ki67 index compared to patients with a lower Ki67 index [42]. We have no explanation for this finding and the number of patients studied is limited. However, it might be possible that even tumors with a high Ki67 index possess high gene expression for SSTR2, but this is not transmitted to protein level. In line with our finding, our findings may question if not peptide receptor radionucleotide therapy (PRRT) e.g. with ^{177}Lu-DOTATATE could, at least from a ligand binding point, be used in high-grade NECs.

The recent focus on personalized medicine has led to a need for tumor characterization and diagnosis at the molecular level [18]. Thus, targeted treatment with mTOR-inhibitors have been shown to prolong progression free survival (PFS) in patients with NEN [43, 44]. Therefore, we investigated if a potential marker for phosphatidylinositol 3-kinase (PIK3)/protein kinase B (AKT)/mTOR pathway activation might be detectable in NEC to select patients who could profit from a therapy with a mTOR-inhibitor. Protein mTOR was only expressed in 14% of cases (n=3; **Table 2**) having a primary tumor origin in pancreas, rectum or cancer of unknown primary (CUP). Positive IHC reactivity of mTOR has been suggested as a negative prognostic marker in NENs with low Ki67 indices, but is not validated in a cohort of NEC and cannot be compared with the present study [26]. Interestingly, the gene expression levels of SSTR2 and mTOR were significantly positively correlated ($p=0.013$). The hyper-activation of the PIK3/AKT/mTOR signaling pathway promotes resistance to cell death and is an important target for cancer therapy [44, 45]. A proposal of dual targeting with an mTOR-inhibitor and SST-analog in treatment of advanced NEN associated with carcinoid syndrome has been proposed [43, 46]. The rationale for this approach is that the SST-analog binds to SSTR2 on the cell surface, leading to reduced hormone secretion by inhibiting cyclic adenosine monophosphate and intracellular calcium, causing increased apoptosis, and/or to reduced cell proliferation by activating protein tyrosine phosphatases and subsequent regulation of different intracellular pathways including the PIK3/AKT/mTOR [45, 47]. The results of the present study reflect the association between SSTR2 and mTOR and the presence of mTOR on RNA level. At the protein level mTOR is not explicit in our study, hence it had been advantageous if a comprehensive IHC work-up of the PIK3/AKT/mTOR pathway had been performed on both RNA and protein level, since mTOR might not be the correct target in this pathway.

Related to the mTOR complex is the angiogenic pathway mediated by the vascular endothelial growth factor A (VEGFA) and the hypoxia-inducible factor (HIF1α) which both have a role in the

carcinogenesis of NENs [45]. The transcription factor, HIF1α, controls the expression of downstream proteins including VEGFA and carbonic anhydrase 9 (CA-IX) whose role is to stimulate tumor cell proliferation in conditions of hypoxic conditions, ultimately promoting angiogenesis, local invasion and metastasis [48]. Cell adhesion molecules as integrin-α_V (ITGAV) and integrin-β_3 (ITGB3) are presumed to be indicators of neo-angiogenesis and are expressed at variable levels in NENs [49]. Since a promising angiogenesis PET-tracer (^{64}Cu-NODAGA-c(RGDyK)) targeting above mentioned integrins has been presented, and the fact that anti-angiogenetic therapy is currently explored in NENs in several clinical trials (e.g. bevacizumab, ID#NCT01121939; sunitinib, ID#NCT-01525550) we found it relevant to investigate the different markers involved in angiogenesis [45, 50]. Earlier publications have suggested an interplay of SSTR signaling and hypoxia and since angiogenesis is a pathogenic hallmark as well as a therapeutic target we aimed to investigate tissue markers of hypoxia and angiogenesis, however we did not find any correlation of HIF1α, VEGFA, CA-IX, ITGAV or ITGB3 on messenger RNA (mRNA) level to either SRI-uptake or SSTR2 gene expression [45, 48, 51].

uPAR has been shown to be up-regulated during neoplastic invasion, and metastatic development and may predict more aggressive phenotypes [33]. In this study 76% of the cases had positive IHC uPAR (**Table 2**). This study supports the theory of uPAR being expressed in aggressive phenotypes, moreover uPAR could be of interest as a target by non-invasive PET imaging in a variety of tumors [52-58].

To obtain a profound understanding of NECs, future studies should emphasize the gene expression pattern in NECs resulting in a more individualized approach on a diagnostic as well as therapeutic level. Moreover, there is a strong need for identifying novel prognostic factors capable of predicting the biological behavior of the disease.

One limitation is the rather limited number of patients. However, due to the restricted number of NEC patients who underwent surgery and the limited availability of fresh-frozen tissue, the presented material is unique and demonstrates substantial differences in markers fundamental for SRI. In accordance with this we did indeed demonstrate a highly significant correlation between ^{68}Ga-DOTATOC PET tracer uptake and gene expression of SSTR2.

Acknowledgements

The economical support from the John and Birthe Meyer Foundation, the Capital region of Denmark, Rigshospitalets Research Council, Svend Andersen Foundation, the Arvid Nilsson Foundation, the Innovation Fund, the Novo Nordisk Foundation and the Lundbeck Foundations is acknowledged. The authors wish to thank Michelle Kaijer for assistance on IHC (Cluster of Molecular Imaging, University of Copenhagen, Rigshospitalet, Denmark) and the staff of the Dept. of Clinical Physiology, Nuclear Medicine & PET (Rigshospitalet, Denmark) for performing the scans.

Disclosure of conflict of interest

The authors declare no conflict of interest.

Address correspondence to: Dr. Andreas Kjaer, Department of Clinical Physiology, Nuclear Medicine & PET, KF-4012, Rigshospitalet, National University Hospital, Blegdasmvej 9, DK-2100 Copenhagen, Denmark. E-mail: akjaer@sund.ku.dk

References

[1] Bosman F, Carneiro F, Hruban R. WHO Classification of Tumours of the Digestive System. 4th ed. Lyon, France. IARC Press; 2010.

[2] Oberg K, Hellman P, Ferolla P, Papotti M; ESMO Guidelines Working Group. Neuroendocrine bronchial and thymic tumors: ESMO Clinical Practice Guidelines for diagnosis, treatment and follow-up. Ann Oncol 2012; 23: 120-23.

[3] Phan AT, Oberg K, Choi J, Harrison LH, Hassan MM, Strosberg JR, Krenning EP, Kocha W, Woltering EA, Maples WJ. NANETS consensus guideline for the diagnosis and management of neuroendocrine tumors: well-differentiated neuroendocrine tumors of the thorax (includes lung and thymus). Pancreas 2010; 39: 784-98.

[4] Oberg K, Knigge U, Kwekkeboom D, Perren A; ESMO Guidelines Working Group. Neuroendocrine gastro-entero-pancreatic tumors: ESMO Clinical Practice Guidelines for diagnosis, treatment and follow-up. Ann Oncol 2012; 23: 124-30.

[5] Basturk O, Tang L, Hruban RH, Adsay V, Yang Z, Krasinskas AM, Vakiani E, La Rosa S, Jang KT, Frankel WL, Liu X, Zhang L, Giordano TJ, Bellizzi AM, Chen JH, Shi C, Allen P, Reidy DL, Wolfgang CL, Saka B, Rezaee N, Deshpande V, Klimstra

DS. Poorly differentiated neuroendocrine carcinomas of the pancreas: a clinicopathologic analysis of 44 cases. Am J Surg Pathol 2014; 38: 437-47.

[6] Ilett E, Langer S, Olsen I, Federspiel B, Kjær A, Knigge U. Neuroendocrine Carcinomas of the Gastroenteropancreatic System: A Comprehensive Review. Diagnostics 5: 119-76.

[7] Sorbye H, Welin S, Langer S, Vestermark L, Holt N, Osterlund P, Dueland S, Hofsli E, Guren MG, Ohrling K, Birkemeyer E, Thiis-Evensen E, Biagini M, Gronbaek H, Soveri LM, Olsen IH, Federspiel B, Assmus J, Janson ET, Knigge U. Predictive and prognostic factors for treatment and survival in 305 patients with advanced gastrointestinal neuroendocrine carcinoma (WHO G3): The NORDIC NEC study. Ann Oncol 2012; 24: 152-160.

[8] Janson ET, Sorbye H, Welin S, Federspiel B, Grønbaek H, Hellman P, Ladekarl M, Langer SW, Mortensen J, Schalin-Jäntti C, Sundin A, Sundlöv A, Thiis-Evensen E, Knigge U. Nordic guidelines 2014 for diagnosis and treatment of gastroenteropancreatic neuroendocrine neoplasms. Acta Oncol 2014; 53: 1284-1297.

[9] Modlin IM, Pavel M, Kidd M, Gustafsson BI. Review article: somatostatin analogues in the treatment of gastroenteropancreatic neuroendocrine (carcinoid) tumours. Aliment Pharmacol Ther 2010; 31: 169-88.

[10] de Herder WW, Hofland LJ, van der Lely AJ, Lamberts SW. Somatostatin receptors in gastroentero-pancreatic neuroendocrine tumours. Endocr Relat Cancer 2003; 10: 451-458.

[11] Rinke A, Müller HH, Schade-Brittinger C, Klose KJ, Barth P, Wied M, Mayer C, Aminissadati B, Pape UF, Bläker M, Harder J, Arnold C, Gress T, Arnold R; PROMID Study Group. Placebo-controlled, double-blind, prospective, randomized study on the effect of octreotide LAR in the control of tumor growth in patients with metastatic neuroendocrine midgut tumors: a report from the PROMID Study Group. J Clin Oncol 2009; 27: 4656-63.

[12] Caplin ME, Pavel M, Ćwikła JB, Phan AT, Raderer M, Sedláčková E, Cardiot G, Wolin EM, Capdevila J, Wall L, Rindi G, Langley, Martinez S, Blumberg J, Ruszniewski P; CLARINET Investigators. Lanreotide in metastatic enteropancreatic neuroendocrine tumors. N Engl J Med 2014; 371: 224-33.

[13] Fischer T, Doll C, Jacobs S, Kolodziej A, Stumm R, Schulz S. Reassessment of sst2 somatostatin receptor expression in human normal and neoplastic tissues using the novel rabbit monoclonal antibody UMB-1. J Clin Endocrinol Metab 2008; 93: 4519-24.

[14] Oberg KE, Reubi JC, Kwekkeboom DJ, Krenning EP. Role of somatostatins in gastroenteropancreatic neuroendocrine tumor development and therapy. Gastroenterology 2010; 139: 742-53.

[15] Pfeifer A, Knigge U, Mortensen J, Oturai P, Berthelsen AK, Loft A, Binderup T, Rasmussen P, Elema D, Klausen TL, Holm S, von Benzon E, Højgaard L, Kjaer A. Clinical PET of Neuroendocrine Tumors Using 64Cu-DOTATATE: First-in-Humans Study. J Nucl Med 2012; 53: 1207-15.

[16] Chalabi M, Duluc C, Caron P, Vezzosi D, Guillermet-Guibert J, Pyronnet S, Bousquet C. Somatostatin analogs: does pharmacology impact antitumor efficacy? Trends Endocrinol Metab 2014; 25: 115-27.

[17] Pfeifer A, Knigge U, Binderup T, Mortensen J, Oturai P, Loft A, Berthelsen AK, Langer SW, Rasmussen P, Elema D, von Benzon E, Højgaard L, Kjaer A. 64Cu-DOTATATE PET for Neuroendocrine Tumors: A Prospective Head-to-Head Comparison with 111In-DTPA-Octreotide in 112 Patients. J Nucl Med 2015; 56: 847-54.

[18] Kjær A, Knigge U. Use of radioactive substances in diagnosis and treatment of neuroendocrine tumors. Scand J Gastroenterol 2015; 50: 740-7.

[19] Kaemmerer D, Peter L, Lupp A, Schulz S, Sänger J, Prasad V, Kulkarni H, Haugvik SP, Hommann M, Baum RP. Molecular imaging with 68Ga-SSTR PET/CT and correlation to immunohistochemistry of somatostatin receptors in neuroendocrine tumours. Eur J Nucl Med Mol Imaging 2011; 38: 1659-68.

[20] Binderup T, Knigge U, Mellon Mogensen A, Palnaes Hansen C, Kjær A. Quantitative gene expression of somatostatin receptors and noradrenaline transporter underlying scintigraphic results in patients with neuroendocrine tumors. Neuroendocrinology 2008; 87: 223-32.

[21] Janson ET, Stridsberg M, Gobl A, Westlin JE, Oberg K. Determination of somatostatin receptor subtype 2 in carcinoid tumors by immunohistochemical investigation with somatostatin receptor subtype 2 antibodies. Cancer Res 1998; 58: 2375-8.

[22] Volante M, Brizzi MP, Faggiano A, La Rosa S, Rapa I, Ferrero A, Mansueto G, Righi L, Garancini S, Capella C, De Rosa G, Dogliotti L, Colao A, Papotti M. Somatostatin receptor type 2A immunohistochemistry in neuroendocrine tumors: a proposal of scoring system correlated with somatostatin receptor scintigraphy. Mod Pathol 2007; 20: 1172-82.

[23] Komori Y, Yada K, Ohta M, Uchida H, Iwashita Y, Fukuzawa K, Kashima K, Yokoyama S, Inomata M, Kitano S. Mammalian target of rapamycin signaling activation patterns in pancreatic neuroendocrine tumors. J Hepatobiliary Pancreat Sci 2014; 21: 288-95.

[24] Ghayee HK, Giubellino A, Click A, Kapur P, Christie A, Xie XJ, Martucci V, Shay JW, Souza RF, Pacak K. Phospho-mTOR is not upregulated in metastatic SDHB paragangliomas. Eur J Clin Invest 2013; 43: 970-7.

[25] Kasajima A, Pavel M, Darb-Esfahani S, Noske A, Stenzinger A, Sasano H, Dietel M, Denkert C, Röcken C, Wiedenmann B, Weichert W. mTOR expression and activity patterns in gastroenteropancreatic neuroendocrine tumours. Endocr Relat Cancer 2011; 18: 181-92.

[26] Qian ZR, Ter-Minassian M, Chan JA, Imamura Y, Hooshmand SM, Kuchiba A, Morikawa T, Brais LK, Daskalova A, Heafiel R, Lin X, Christiani DC, Fuchs CS, Ogino S, Kulke MH. Prognostic significance of MTOR pathway component expression in neuroendocrine tumors. J Clin Oncol 2013; 31: 3418-25.

[27] Righi L, Volante M, Rapa I, Tavaglione V, Inzani F, Pelosi G, Papotti M. Mammalian target of rapamycin signaling activation patterns in neuroendocrine tumors of the lung. Endocr Relat Cancer 2010; 17: 977-87.

[28] Annaratone L, Volante M, Asioli S, Rangel N, Bussolati G. Characterization of neuroendocrine tumors of the pancreas by real-time quantitative polymerase chain reaction. A methodological approach. Endocr Pathol 2013; 24: 83-91.

[29] Shida T, Kishimoto T, Furuya M, Nikaido T, Koda K, Takano S, Kimura F, Shimizu H, Yoshidome H, Ohtsuka M, Tanizawa T, Nakatani Y, Miyazaki M. Expression of an activated mammalian target of rapamycin (mTOR) in gastroenteropancreatic neuroendocrine tumors. Cancer Chemother Pharmacol 2010; 65: 889-93.

[30] Ruza A, Griniak K, Phillip L, Felder S, Pape UF, Manfred D. Immunohistochemical Analysis of mTOR Pathway Expression in Gastric Neuroendocrine Tumors. J Clin Exp Pathol 2014; 4: 1-6.

[31] Rønne E, Høyer-Hansen G, Brünner N, Pedersen H, Rank F, Osborne CK, Clark GM, Danø K, Grøndahl-Hansen J. Urokinase receptor in breast cancer tissue extracts. Enzyme-linked immunosorbent assay with a combination of mono- and polyclonal antibodies. Breast Cancer Res Treat 1995; 33: 199-207.

[32] Alpízar-Alpízar W, Nielsen BS, Sierra R, Illemann M, Ramírez JA, Arias A, Durán S, Skarstein A, Ovrebo K, Lund LR, Laerum OD. Urokinase plasminogen activator receptor is expressed in invasive cells in gastric carcinomas from high- and low-risk countries. Int J Cancer 2010; 126: 405-15.

[33] Alpízar-Alpízar W, Christensen IJ, Santoni-Rugiu E, Skarstein A, Ovrebo K, Illemann M, Laerum OD. Urokinase plasminogen activator receptor on invasive cancer cells: a prognostic factor in distal gastric adenocarcinoma. Int J Cancer 2012; 131: E329-36.

[34] Boonstra MC, Verbeek FP, Mazar AP, Prevoo HA, Kuppen PJ, van de Velde CJ, Vahrmeijer AL, Sier CF. Expression of uPAR in tumor-associated stromal cells is associated with colorectal cancer patient prognosis: a TMA study. BMC Cancer 2014; 14: 269.

[35] Magnussen S, Rikardsen OG, Hadler-Olsen E, Uhlin-Hansen L, Steigen SE, Svineng G. Urokinase plasminogen activator receptor (uPAR) and plasminogen activator inhibitor-1 (PAI-1) are potential predictive biomarkers in early stage oral squamous cell carcinomas (OSCC). PLoS One 2014; 9: e101895.

[36] Li P, Gao Y, Ji Z, Zhang X, Xu Q, Li G, Guo Z, Zheng B, Guo X. Role of urokinase plasminogen activator and its receptor in metastasis and invasion of neuroblastoma. J Pediatr Surg 2004; 39: 1512-9.

[37] Hellemans J, Mortier G, De Paepe A, Speleman F, Vandesompele J. qBase relative quantification framework and software for management and automated analysis of real-time quantitative PCR data. Genome Biol 2007; 8: R19.

[38] Vandesompele J, De Preter K, Pattyn F, Poppe B, Van Roy N, De Paepe A, Speleman F. Accurate normalization of real-time quantitative RT-PCR data by geometric averaging of multiple internal control genes. Genome Biol 2002; 3.

[39] Virgolini I, Ambrosini V, Bomanji JB, Baum RP, Fanti S, Gabriel M, Papathanasiou ND, Pepe G, Oyen W, De Cristoforo C, Chiti A. Procedure guidelines for PET/CT tumour imaging with 68Ga-DOTA-conjugated peptides: 68Ga-DOTA-TOC, 68Ga-DOTA-NOC, 68Ga-DOTA-TATE. Eur J Nucl Med Mol Imaging 2010; 37: 2004-10.

[40] Papotti M, Bongiovanni M, Volante M, Allìa E, Landolfi S, Helboe L, schindler M, Cole SL, Bussolati G. Expression of somatostatin receptor types 1-5 in 81 cases of gastrointestinal and pancreatic endocrine tumors. A correlative immunohistochemical and reverse-transcriptase polymerase chain reaction analysis. Virchows Arch 2002; 440: 461-75.

[41] Johnbeck CB, Knigge U, Kjær A. PET tracers for somatostatin receptor imaging of neuroendocrine tumors: current status and review of the literature. Future Oncol 2014; 10: 2259-77.

[42] Binderup T, Knigge U, Loft A, Mortensen J, Pfeifer A, Federspiel B, Hansen CP, Højgaard L, Kjaer A. Functional Imaging of Neuroendocrine Tumors: A Head-to-Head Comparison of Somatostatin Receptor Scintigraphy, 123I-MIBG Scintigraphy, and 18F-FDG PET. J Nucl Med 2010; 51: 704-12.

[43] Pavel ME, Hainsworth JD, Baudin E, Peeters M, Hörsch D, Winkler RE, Klimovsky J, Lebwohl D, Jehl V, Wolin EM, Oberg K, Van Cutsem E, Yao JC; RADIANT Study Group. Everolimus plus oc-

treotide long-acting repeatable for the treatment of advanced neuroendocrine tumours associated with carcinoid syndrome (RADIANT-2): a randomised, placebo-controlled, phase 3 study. Lancet 2011; 378: 2005-12.

[44] Yao JC, Shah MH, Ito T, Bohas CL, Wolin EM, Van Cutsem E, Hobday TJ, Okusaka T, Capdevila J, de Vries EG, Tomassetti P, Pavel ME, Hoosen S, Haas T, Lincy J, Lebwohl D, Öberg K. Everolimus for advanced pancreatic neuroendocrine tumors. N Engl J Med 2011; 364: 514-23.

[45] Walenkamp A, Crespo G, Fierro Maya F, Fossmark R, Igaz P, Rinke A, Tamagno G, Vitale G, Öberg K, Meyer T. Hallmarks of gastrointestinal neuroendocrine tumours: implications for treatment. Endocr Relat Cancer 2014; 21: R445-60.

[46] Yao JC, Lagunes DR, Kulke MH. Targeted therapies in neuroendocrine tumors (NET): clinical trial challenges and lessons learned. Oncologist 2013; 18: 525-32.

[47] Chalabi M, Duluc C, Caron P, Vezzosi D, Guillermet-Guibert J, Pyronnet S, Bousquet C. Somatostatin analogs: does pharmacology impact antitumor efficacy? Trends Endocrinol Metab 2014; 25: 115-27.

[48] Pinato DJ, Tan TM, Toussi ST, Ramachandran R, Martin N, Meeran K, Ngo N, Dina R, Sharma R. An expression signature of the angiogenic response in gastrointestinal neuroendocrine tumours: correlation with tumour phenotype and survival outcomes. Br J Cancer 2014; 110: 115-22.

[49] Oxboel J, Binderup T, Knigge U, Kjær A. Quantitative gene-expression of the tumor angiogenesis markers vascular endothelial growth factor, integrin alphaV and integrin beta3 in human neuroendocrine tumors. Oncol Rep 2009; 21: 769-75.

[50] Oxboel J, Schjoeth-Eskesen C, El-Ali H, Madsen J, Kjaer A. (64)Cu-NODAGA-c(RGDyK) Is a Promising New Angiogenesis PET Tracer: Correlation between Tumor Uptake and Integrin α(V)β(3) Expression in Human Neuroendocrine Tumor Xenografts. Int J Mol Imaging 2011; 2012: 379807.

[51] Villaume K, Blanc M, Gouysse G, Walter T, Couderc C, Nejjari M, Vercherat C, Cordier-Bussat M, Roche C, Scoazec JY. VEGF secretion by neuroendocrine tumor cells is inhibited by octreotide and by inhibitors of the PI3K/AKT/mTOR pathway. Neuroendocrinology 2010; 91: 268-78.

[52] Persson M, Ali El HH, Binderup T, Pfeifer A, Madsen J, Rasmussen P, Kjaer A. Dosimetry of 64Cu-DOTA-AE105, a PET tracer for uPAR imaging. Nucl Med Biol 2014; 41: 290-5.

[53] Persson M, Skovgaard D, Brandt-Larsen M, Christensen C, Madsen J, Nielsen CH, Thurison T, Klausen TL, Holm S, Loft A, Berthelsen AK, Ploug M, Pappot H, Brasso K, Kroman N, Højgaard L, Kjaer A. First-in-human uPAR PET: Imaging of Cancer Aggressiveness. Theranostics 2015; 5: 1303-16.

[54] Persson M, Nedergaard M, Brandt-Larsen M, Skovgaard D, Jørgensen JT, Michaelsen SR, Madsen J, Lassen U, Poulsen HS, Kjaer A. uPAR is a Promising New Imaging Biomarker in Glioblastoma. J Nucl Med 2015; [Epub ahead of print].

[55] Persson M, Hosseini M, Madsen J, Jørgensen TJ, Jensen KJ, Kjaer A, Ploug M. Improved PET imaging of uPAR expression using new (64)Cu-labeled cross-bridged peptide ligands: comparative in vitro and in vivo studies. Theranostics 2013; 3: 618-32.

[56] Persson M, Liu H, Madsen J, Cheng Z, Kjaer A. First (18)F-labeled ligand for PET imaging of uPAR: in vivo studies in human prostate cancer xenografts. Nucl Med Biol 2013; 40: 618-24.

[57] Persson M, Madsen J, Østergaard S, Jensen MM, Jørgensen JT, Juhl K, Lehmann C, Ploug M, Kjaer A. Quantitative PET of human urokinase-type plasminogen activator receptor with 64Cu-DOTA-AE105: implications for visualizing cancer invasion. J Nucl Med 2012; 53: 138-45.

[58] Persson M, Madsen J, Østergaard S, Ploug M, Kjaer A. 68Ga-labeling and in vivo evaluation of a uPAR binding DOTA- and NODAGA-conjugated peptide for PET imaging of invasive cancers. Nucl Med Biol 2012; 39: 560-9.